Journal of Drug Delivery Science and Technology 74 (2022) 103498

Contents lists available at ScienceDirect

Journal of Drug Delivery Science and Technology

journal homepage: www.elsevier.com/locate/jddst

Binary ethosomes-based transdermal patches assisted by metal microneedles significantly improve the bioavailability of carvedilol

Di Jiang [a], Yuxin Jiang [b,c,**], Kaili Wang [a], Zhe Wang [a], Yifei Pei [a], Jinglei Wu [a], Chuanglong He [a], Xiumei Mo [a], Hongsheng Wang [a,*]

[a] Shanghai Engineering Research Center of Nano-Biomaterials and Regenerative Medicine, College of Biological Science and Medical Engineering, Donghua University, Shanghai, 201620, PR China
[b] Jiaxing Key Laboratory of Virus-related Infectious Diseases, The First Hospital of Jiaxing City, Jiaxing University, Jiaxing, 314001, PR China
[c] Department of Pathogenic Biology and Immunology, School of Medicine, Jiaxing University, Jiaxing, 314001, PR China

ARTICLE INFO

Keywords:
Binary ethsomes
Antihypertension
Transdermal drug delivery patches
Microneedles

ABSTRACT

This study aimed to develop a strategy combining binary ethsomes (BES) and microneedles (MNs) to improve the bioavailability of drugs that are poorly bioavailable by oral administration, such as carvedilol (CL). The formula of BES was optimized by Box-Benhnken Designes from four aspects: particle size, zeta potential, encapsulation efficiency and cumulative release in vitro. The optimized BES was then mixed with polyvinylpyrrolidone and sprayed onto the silk fibroin matrix by electrospray to obtain transdermal drug delivery patches (TDDP). In vitro skin penetration test showed that, TDDP has much better transdermal drug release performance compared with free drugs, and MNs-assisted TDDP (MNs-TDDP) can deliver more drugs to the receiving chamber. In vivo studies indicate that MNs-TDDP can significantly reduce the fluctuation of CL concentration in plasma and increase serum level of NO, thereby lower blood pressure for a longer time. These results suggest that the bioavailability of CL can be greatly improved via administration of MNs-TDDP, compared with the oral route. Considering its advantages of non-invasiveness, convenience and good biosafety, MNs-TDDP has a promising prospect in improving the bioavailability of drugs for treating chronic diseases such as hypertension.

1. Introduction

Hypertension is one of the common diseases in today's society and the main risk factor for cardiovascular disease [1,2]. Carvedilol (CL) is a compound with antioxidant properties that is clinically used to treat cardiovascular diseases such as hypertension, congestive heart failure, and myocardial infarction [3]. As a non-selective β receptor blocker, it can block both β_1 receptors and α_1 receptors, and has the effect of dilating peripheral blood vessels [4,5]. CL can be rapidly absorbed by the gastrointestinal tract, but is first absorbed and metabolized in the liver, with an absolute bioavailability of about 25% and a half-life of about 6 h [6]. CL has the characteristics of low relative molecular weight (406.5), appropriate logarithmic partition coefficient, small dosage range, short plasma half-life, and poor oral bioavailability, which means that it is a drug suitable for transdermal delivery [6]. CL can be stably loaded into the transdermal drug delivery patches (TDDP) entering the local subcutaneous capillaries through transdermal administration and effectively released into the internal circulation [7].

In recent years, TDD has become a new subcutaneous drug delivery method [8]. TDD avoids the first pass effect of the liver and gastrointestinal side effects, and reduces the fluctuation of the blood concentration of the drug. However, the stratum corneum (SC), the outermost dense skin layer, limits the human body's absorption of drugs through transdermal administration. Many methods have been researched and developed to increase the permeability of drugs through the stratum corneum [9,10]. It was proposed to reduce the needle to a micron size, to use the powerful delivery capacity of injection and to improve patient compliance at the same time, which led to the invention of microneedles (MNs). MNs have the advantages of no pain or slight pain, multiple administrations, convenient carrying, and low cost [11]. Although metal MNs are highly effective for transdermal drug delivery, their ability to achieve controlled drug release is limited, and such ability is extremely

* Corresponding author.
** Corresponding author. Jiaxing Key Laboratory of Virus-related Infectious Diseases, The First Hospital of Jiaxing City, Jiaxing University, Jiaxing, 314001, PR China.
E-mail address: whs@dhu.edu.cn (H. Wang).

https://doi.org/10.1016/j.jddst.2022.103498
Received 22 January 2022; Received in revised form 22 April 2022; Accepted 10 June 2022
Available online 13 June 2022

beneficial for effective blood pressure control. Biodegradable MNs can overcome the above limitations by adjusting the degradation rate to control the drug release rate, but they are not suitable for chronic diseases such as hypertension that require long-term repeated medication, because the accumulation of dissolved components of microneedle may bring potential risks to the human body [12]. The search for a better strategy is still urgent for transdermal administration of drugs like CL to treat chronic diseases like hypertension.

Ethsomes is a special kind of liposome, which is prepared by adding high-concentration alcohol solution during the preparation process [13]. The binary ethsomes (BES) is an improvement of the ethsomes, prepared by mixing ethanol and propanediol in a certain proportion. Compared with liposomes, BES have good biocompatibility, better stability, intrinsic skin penetration enhancement characteristics, high encapsulation efficiency, large drug loading, and better flexibility [14]. BES can be used as a drug storage library, and its composition or surface modification can adjust the release rate of the drug and the affinity of the target. It can coat lipophilic and hydrophilic drugs, as a local carrier for the sustained release of skin active compounds, and as a penetration enhancer, which can penetrate deep into the skin to promote drug transdermal absorption and aggregation in the skin [15]. Thus, BES is a good carrier for TDD, and the TDDP containing drug-loaded BES may achieve long-term controlled transdermal release. Pinpricking the local skin using metal MNs before administration with the BES-loaded TDDP should be helpful to improve the transdermal efficiency of BES.

We hypothesized that TDDP containing drug-loaded BES assisted by metal MNs may be a useful strategy for the treatment of chronic diseases due to the improved transdermal absorption and bioavailability of the drugs. In this study, the formula of BES was optimized by the method of Box-Benhnken Design (BBD). Using CL as model drug, the CL-loaded BES (CL@BES) were mixed with polyvinyl pyrrolidone (PVP) ethanol solution and electrosprayed onto the surface of silk fibroin matrices (SFM) to prepare TDDP. The skin penetration efficiency of the TDDP was studied with Franz assay in vitro. The pharmacodynamics and antihypertensive effect of the TDDP assisted with MNs were investigated using Wistar-Kyoto rats (WKY) and spontaneously hypertensive rats (SHR) respectively.

2. Materials and methods

2.1. Materials

Carvedilol was procured from Adamas Reagent, Ltd. (Shanghai, China). Lecithin was purchased from A.V.T.(Shanghai) Pharmaceutical Co., Ltd. (Shanghai, China). Cholesterol, octadecylamine,1,1′-dioctadecyl-3,3,3′,3′-tetramethylindocarbocyanine perchlorate (DiI), sodium dodecyl sulfate (SDS), acetonitrile and methanol were purchased from Sigma-Aldrich Trading Co., Ltd. (Shanghai, China). Cocoons were from Huzhou Silk Co., Ltd. (Huzhou, China). Calcium chloride, propanediol and absolute ethanol were from Sinopharm Chemical Reagent Co., Ltd. (Shanghai, China). Phosphate buffer saline (PBS) and PVP was procured from Aladdin Biochemical Technology Co., Ltd. (Shanghai China). Rat nitric oxide (NO) ELISA Kit was purchased from Jinpin Chemical Technology Co., Ltd. (Shanghai, China). Hematoxylin/eosin (H&E) Staining Kit and immunofluorescence transferase-mediated dUTP nick-end labeling (IF-TUNEL) Kit were purchased from Servicebio Co., Ltd. (Wuhan, China). All the chemicals and solvents used were of analytical grade. Microneedle roller (Dermaroller®) with a needle length of 500 μm was purchased from DRS® Dermaroller System (Berlin, Germany). SHR and WKY rats were purchased from Beijing Vital River Laboratory Animal Technology Co. Ltd (Beijing, China).

2.2. Experimental design for formula optimization of BES

2.2.1. Design

A 4^3 full factorial design was employed using Design-Expert 11.0.0 software (Stat-Ease Inc., USA). Four independent formulation variables (lecithin, octadecylamine, ethanol, and propanediol) were studied and their individual and combined effects were evaluated. The effects of particle size, zeta potential, encapsulation efficiency (EE) and cumulative drug release of 24 h (CDR_{24h}) were selected as the dependent variables. The level of the independent variable was determined according to the literature and our previous experiments. The full factorial design including independent variables and dependent variables is shown in Table 1.

Table 1
Independent variables and responses used in BBD for the preparation of BES.

Independent variable	Levels		
	−1	0	+1
A: Lecithin (g)	0.05	0.10	0.15
B: Octadecylamine (g)	0.00	0.01	0.02
C: Ethanol (% v/v)	20	30	40
D: Propanediol (% v/v)	0	5	10
Responses	Desirability constraints		
Y_1: Particle size (nm)	Minimize		
Y_2: Zeta potential (mV)	Maximize		
Y_3: EE	Maximize		
Y_4: CDR_{24h} (μg)	Maximize		

2.2.2. Preparation of BES

BES were prepared by thin-film hydration technique. Briefly, lecithin, cholesterol and octadecylamine were dissolved in absolute ethanol at room temperature and stirred at 400 rpm for 30 min with a magnetic stirrer (Chijiu HO5-1, Shanghai Meiyingpu Instrument Manufacturing Co., Ltd., Shanghai, China). The mixture was transferred into a round-bottom flask and evaporated with a rotary evaporator (ZX98-1, Shanghai Looye Industry and Trade Co., Ltd., Shanghai, China) runing at 40 °C and 5 rpm for 30 min to obtain a lipid film. A mixed solution composed of absolute ethanol, propanediol and deionized water in different proportions was added to dissolve the lipid film by stirring at 100 rpm for 30 min with a magnetic stirrer (Chijiu HO5-1). The mixture was then sonicated to obtain BES with a probe sonicator (JY92-II, NingBo Scientz Biotechnology Co., Ltd., Ningbo, China) under the following condition: power 100W, working time 5s, interval time 3s, 10 cycles. After dyeing the prepared BES with 4% phosphotungstic acid, the morphology of the BES was observed using a transmission electron microscope (TEM, JEM-2100F, jeol, japan). The particle size and zeta potential of BES were determined using Zetasizer Nano ZS (ZEN3600, Malvern Instruments, UK).

2.2.3. Determination of encapsulation efficiency (EE)

The concentration of unentrapped CL in the CL@BES solution was measured at 285 nm by a spectrophotometer (TU-1810, Beijing Purkinje General Insrtument Co., Ltd., Beijing, China). Then, 1% Triton solution and the CL@BES solution were mixed in a volume ratio of 1:1 to cleave the lipid to release the drug in the BES and the CL concentration was determined spectrophotometrically after suitable dilution. Finally, EE of BES to CL was calculated with equation (1).

$$EE = \frac{C_2 - C_1}{C_2} \times 100\% \quad (1)$$

(where C_1 is the concentration of unentrapped CL and C_2 is the concentration of CL after cleaving).

2.2.4. In vitro release study

1.00 mL of CL@BES solution was added to the 3000 Da dialysis bag, PBS (pH = 7.4) containing 0.50% (wt/v) SDS (SDS-PBS) was used as the release medium. The drug release experiment was performed in a 37 °C constant temperature oscillator. 2.00 mL dialysate was withdrawn at different time point (2, 4, 6, 8, 10, 12, and 24 h) and an equal volume of fresh release medium was supplemented immediately. The extracted

samples were analyzed at 285 nm by a spectrophotometer (TU-1810) and the CDR of CL was calculated according to equation (2).

$$Q = VC_n + \sum_{i=1}^{n-1} V_i C_i \quad (2)$$

(where Q is the cumulative amount of CL transdermal released, V is the total volume of the receiving chamber, C_n is the concentration of CL at n sampling time, V_i is the volume at i sampling time, and C_i is the concentration of CL at i sampling time).

2.3. Preparation and characterization of the transdermal drug delivery patches (TDDP)

The silkworm cocoon shells were soaked in the $CaCl_2$-ethanol-H_2O (mass ratio = 1:2:8) ternary solution and incubated at 90 °C for overnight. After rinsing with 50% ethanol aqueous solution to remove residual Ca^{2+}, SFM was obtained. PVP was dissolved in 60% ethanol aqueous solution, then mixed with BES and the mixture was electrospayed onto the surface of the dried SFM to obtain TDDP under the following conditions: voltage 18 kV, extrusion rate 1 mL/h, receiving distance 15 cm, temperature 40 °C, humidity 8%. The morphology of TDDP was observed by scanning electron microscopy (SEM, Phenom XL, Phenom Scientific, Shanghai, China). The mechanical performance of TDDP was tested by a tensile testing machine (HY940-FS, Shanghai Hengyu Instrument Co., Ltd, China). The hydrophilicity of TDDP was detected with the method of droplet angle measurement using an Angle measuring instrument (DSA30 Kruss, Germany). TDDP was also characterized by infrared spectroscopy in the range of 400–4000 cm^{-1} with a spectrometer (Nicolet 6700, Thermo fisher, USA).

2.4. In vitro study on skin permeation of TDDP

In vitro skin penetration studies were carried out using Franz diffusion cells with an effective diffusion area of 1.30 cm^2. The receiving pool was filled with SDS-PBS, and stirred continuously by a magnetic bar at 120 rpm while maintaining at 33.00 °C ± 0.10 in water bath. A commercially available microneedle roller (Dermaroller®) with a needle length of 500 μm was used to increase the penetration efficiency of BES. The dermis layer of the skin faces upward to the supply chamber, and is attached to the TDDP containing DiI-labeled BES. 2.00 mL receiving fluid was taken at different time point (2, 4, 6, 8, 10, 12 and 24 h) and an equal volume of the fresh one was supplemented to maintain the volume constant. The withdrawn samples were analyzed at 285 nm with a spectrophotometer (TU-1810). The cumulative transdermal release amount of CL was calculated according to equation (2), and the steady-state flux ($Jss_{(2-24h)}$) was calculated with equation (3). The above tested skin tissue samples were also made into paraffin-embedded sections and stained with H&E to observe the epidermal structure as well as the distribution of BES in the skin using a microscope (DMi 8, Leica Microsystems Ltd., Wetzlar, Germany).

$$Jss_{(2-24h)} = \frac{\Delta Q_t}{\Delta t \times S} \quad (3)$$

(where ΔQ_t is the cumulative drug penetration within a certain period of time (Δt), and S is the diffusion area).

2.5. Animal experiments

The animals were maintained in a 12 h light/dark cycle with free access to food and water (SPF environment). All animal experiments were performed according to the guidelines approved by the Institutional Animal Care and Use Committee at Donghua University.

2.5.1. Pharmacokinetics study

The pharmacokinetics of male WKY rats was studied to compare the absorption of TDDP and oral drug solution. Rats were housed in animal facilities under standard laboratory conditions prior to experimentation. Fifty rats were randomly divided into two groups: tested and contol. For the tested group, the rats were pinpricked with MNs on the back skin followed by application of TDDP after hairs was cut off. For the control group, rats were taken orally with a dispersion of commercially available CL tablets. Blood was obtained from the orbit of the rat at different time points after the administration. The blood samples were centrifuged at 4000 rpm for 10 min at 4 °C to obtain plasma, which were then stored at −20 °C in labeled tubes for later analysis of high performance liquid chromatography (HPLC). The quantitative determination of CL in plasma was performed by a validated HPLC method, using methanol aqua solution (60%): acetonitrile = 88:12 as a mobile phase delivered at 1.00 mL/min. The HPLC system equipped with pump (LC 2130, SHIMADZU, Japan), UV detector (LC 2030, SHIMADZU, Japan), organizer (LC 2050, SHIMADZU, Japan), chromatography workstation (T2100P, Techcomp Insrtument Co., Ltd., Shanghai, China) and column thermostat (DT-230A, Techcomp Insrtument Co., Ltd., Shanghai, China). The column oven temperature was kept at 40 °C and the peak response was monitored at a wavelength of 242 nm. Manually injecting 20.00 μL of each sample to detect drug concentration in plasma.

2.5.2. Assays to assess the anti-hypertensive effect of TDDP

Fifteen male SHR rats who were over 8 weeks old and weigh about 180 g with stable blood pressure were randomly divided into three groups: MNs-TDDP treated SHR (abbreviated as MNs-TDDP), TDDP treated SHR (abbreviated as TDDP), and untreated SHR (used as positive control). The untreated WKY rats (abbreviated as untreated WKY) were used as negative control. Animals in each group were raised under the same conditions to ensure their food and drinking water. For the group of MNs-TDDP, MNs and TDDP were applied to the back skin of the rats as described above. For the group of TDDP, only TDDP was used. While rats of the two control groups received no treatment after their hairs on back were shaved. The blood pressure of rats in each group at 0, 1, 2, 4, 6, 8, 10, 12, and 24 h was measured by the tail-cuff method with a non-invasive blood pressure measurement system (ZL-620-F, Yaokun, Anhui, China). After the measurement was completed, blood was collected from the rat orbit and placed at room temperature for 2 h. The serum samples were then obtained by centrifugating at 3000 rpm for 10 min at 4 °C. Subsequently, the NO content in the serum was detected with the ELISA kit.

2.5.3. Biosafety evaluation

After the treatment with TDDP or MNs-TDDP, the rats were sacrificed by cervical dislocation. The organs (heart, liver, spleen, lung, and kidney) were taken out and made into sections after being fixed with 4% paraformaldehyde solution. The sections were then stained with H&E or IF-TUNEL and observed under a microscope (DMi 8).

2.6. Statistical analysis

All data were reported as mean ± standard deviation. Statistical analysis was conducted using the one-way analysis of variance (ANOVA) with Tukey's post hoc test or unpaired *t*-test. A *p*-value < 0.05 was considered significant, and the data were indicated with * for $p < 0.05$, ** for $p < 0.01$, *** for $p < 0.001$ and **** for $p < 0.0001$.

3. Results

3.1. Optimization of BES formulations

Response surface method design is a statistical test method that evaluates the influence of each factor on the target variables through experimental design, establishment of models and data analysis to determine the best combination of each factor. This experiment selected four independent variables and four dependent variables. The following

Table 2
BBD responses of BES formulation (means ± SD, n = 3).

Code	A	B	C	D	Y_1	Y_2	Y_3	Y_4
1	0.05	0.00	30	5	335.80 ± 19.69	6.50 ± 0.87	56.84 ± 2.58	224.50 ± 18.20
2	0.15	0.00	30	5	780.10 ± 17.30	3.98 ± 0.49	93.32 ± 4.79	377.92 ± 47.85
3	0.05	0.02	30	5	243.20 ± 15.00	16.20 ± 0.78	71.81 ± 1.83	266.51 ± 28.81
4	0.15	0.02	30	5	726.80 ± 18.42	13.70 ± 0.65	90.61 ± 2.12	456.06 ± 52.69
5	0.10	0.01	20	0	479.40 ± 12.06	11.00 ± 1.07	83.88 ± 2.00	301.25 ± 44.62
6	0.10	0.01	40	0	359.10 ± 38.70	10.80 ± 0.70	70.28 ± 0.85	346.23 ± 23.12
7	0.10	0.01	20	10	506.50 ± 50.85	11.30 ± 1.00	73.50 ± 2.51	361.04 ± 38.91
8	0.10	0.01	40	10	345.90 ± 28.30	10.40 ± 0.50	80.92 ± 1.61	314.40 ± 49.67
9	0.05	0.01	30	0	332.00 ± 20.09	11.00 ± 0.98	68.36 ± 0.30	181.32 ± 38.44
10	0.15	0.01	30	0	632.80 ± 29.72	10.40 ± 0.58	82.68 ± 3.80	459.24 ± 57.76
11	0.05	0.01	30	10	274.20 ± 6.37	9.93 ± 0.84	60.13 ± 3.60	264.71 ± 34.76
12	0.15	0.01	30	10	810.90 ± 28.16	9.56 ± 0.39	86.75 ± 3.82	437.23 ± 47.50
13	0.10	0.00	20	5	373.20 ± 32.51	6.38 ± 1.10	74.21 ± 2.49	291.77 ± 50.19
14	0.10	0.02	20	5	426.20 ± 29.34	14.00 ± 0.81	80.17 ± 0.84	341.73 ± 57.85
15	0.10	0.00	40	5	368.70 ± 23.63	3.79 ± 1.18	82.82 ± 3.41	335.23 ± 49.39
16	0.10	0.02	40	5	596.30 ± 18.60	12.80 ± 0.45	71.35 ± 3.60	324.84 ± 59.74
17	0.05	0.01	20	5	258.10 ± 11.94	10.70 ± 0.51	72.58 ± 3.46	233.98 ± 23.89
18	0.15	0.01	20	5	866.70 ± 6.51	10.80 ± 0.80	83.40 ± 4.61	479.17 ± 43.49
19	0.05	0.01	40	5	234.50 ± 13.26	12.50 ± 1.27	71.96 ± 2.40	229.11 ± 34.55
20	0.15	0.01	40	5	862.90 ± 10.10	10.10 ± 0.64	86.00 ± 1.60	471.14 ± 60.77
21	0.10	0.00	30	0	476.50 ± 16.96	4.79 ± 0.30	82.51 ± 2.90	329.41 ± 43.21
22	0.10	0.02	30	0	548.00 ± 23.69	15.00 ± 0.85	74.80 ± 2.39	318.41 ± 53.58
23	0.10	0.00	30	10	557.20 ± 25.10	5.78 ± 0.38	76.13 ± 0.21	279.72 ± 40.60
24	0.10	0.02	30	10	403.80 ± 18.41	13.70 ± 0.87	73.09 ± 0.36	306.85 ± 32.55
25	0.10	0.01	30	5	519.60 ± 38.20	8.98 ± 0.89	76.89 ± 0.86	345.68 ± 26.38

Notes: A = Lecithin (g); B = Octadecylamine (g); C = Ethanol (% v/v); D = Propanediol (% v/v); Y_1 = Particle size (nm); Y_2 = Zeta potential (mV); Y_3 = EE; Y_4 = CDR_{24h} (μg).

are the results and analysis of each response value. Table 2 shows the BBD experimental design and results of the BES formulation, and Fig. 1 shows the three-dimensional response plot of the four response values.

3.1.1. Effect of independent variables on particle size

The particle size is one of the important physical properties of the BES, and it is also an important factor that affects the transdermal effect of the BES and the release of drugs. The polydiseperse Index (PDI) in dynamic light scattering, or relative deviation, is an important indicator of dispersion. The prepared BES shows a polycystic spherical structure and the particle size of the blank BES is 103.13 ± 21.99 nm, while that of the CL@BES can be much larger (Fig. 2A and B). CL@BES have a particle size range of 234.5 ± 13.26–866.7 ± 6.51 nm. The polynomial equation of the model expressed by the coding factor is as follows:

$$Y_1 = +519.60 + 250.20A + 4.40B\text{-}11.89C + 5.89D + 9.82AB + 4.95AC + 58.98AD + 43.65BC - 56.23BD - 10.08CD + 43.33A^2 - 21.94B^2 - 41.73C^2 - 35.63D^2;\ R^2 = 0.8998$$

Linear term A (lecithin dosage, $p < 0.001$) has a significant effect on the size of vesicles. The positive sign of the coefficient A of the linear term proves the positive effect of the dosage of lecithin on the response value Y_1. With the increase in the dosage of lecithin, the vesicle size also gradually increased. As the main lipid component of BES, the increase in the dosage of lecithin increases the chain length of the lipid bilayer of the BES. And the spatially distributed vesicles are tightly packed, which makes them more likely to merge into a whole, geting a new vesicle with a larger volume to maintain the thermodynamic stability of the original space. In addition, the increase of lecithin will increase the viscosity of the solution [16]. During ultrasound and filtration, it is more difficult to make the size of the ethosomes uniform, and it is also difficult to reduce its size. It has been reported that ethanol increases the elasticity of the BES by fluidizing the phospholipid bilayer, that is, ethanol interacts with the polar head groups of the phospholipids to reduce the melting point of the lipid, thereby increasing the fluidity of the lipid [17]. Among the metabolites, propanediol has a high viscosity, and the coexistence of ethanol and propanediol can increase the stability of the structure of the metabolites, so that the particle size of the metabolites becomes larger [18].

3.1.2. Effect of independent variables on zeta potential

Zeta potential is the main manifestation of the charged properties of the particles. It is known from the literature that liposomes without alcohol are positively charged, and the addition of ethanol will weaken their electrical properties [19]. When the ethanol content reaches 30%, the prepared ethosomes are negatively charged. The BES prepared in this study contained octadecylamine, so that they are positively charged, and the potential is between 3.79 ± 1.18–16.20 ± 0.78 mV. The repulsive effect of the same charge makes the particles move away from each other, reducing aggregation and fusion, and increasing the stability of the entire system. The polynomial equation of the model expressed by the coding factor is as follows:

$$Y_2 = +8.98 - 0.6908A + 4.52B - 0.3158C - 0.1933D + 0.0050AB - 0.6250AC + 0.0575AD + 0.3475BC - 0.5725BD - 0.1750CD + 0.9683A^2 - 0.1254B^2 + 0.8683C^2 + 0.7546D^2;\ R^2 = 0.9656$$

Linear term A (lecithin dosage, $p < 0.05$) and linear term B (octadecylamine dosage, $p < 0.0001$) have a significant impact on the level of potential. The negative sign of the linear term coefficient A proves the negative influence of the dosage of lecithin on the response value Y_2, and the positive sign of the linear term coefficient B proves the positive influence of the octadecylamine dosage on the response value Y_2. According to the polynomial equation, the influence of the linear term coefficient B on electric potential is almost decisive. Lecithin is the main component of ethosomes. The alcohols are negatively charged, the positive charge of the BES is brought by octadecylamine. Therefore, more octadecylamine is used, more positive charge; the more lecithin is used, the more alcohol in the system and the weaker the positive charge [20]. Octadecylamine is mainly combined with lecithin to stably exist in ethosomes, the addition of alcohol affects such combination and weakened the positive charge [21].

3.1.3. Effect of independent variables on entrapment efficiency

Encapsulation rate refers to the percentage of the encapsulated drug in the total dissolved drug. It is an important indicator of the nanomedicine system. It reflects the degree of drug encapsulation by the carrier and is also the basis for further experiments. The encapsulation efficiency of the prepared BES is between 56.84 ± 2.58% and 95.21 ± 4.79%. The polynomial equation of the model expressed by the coding factor is as follows:

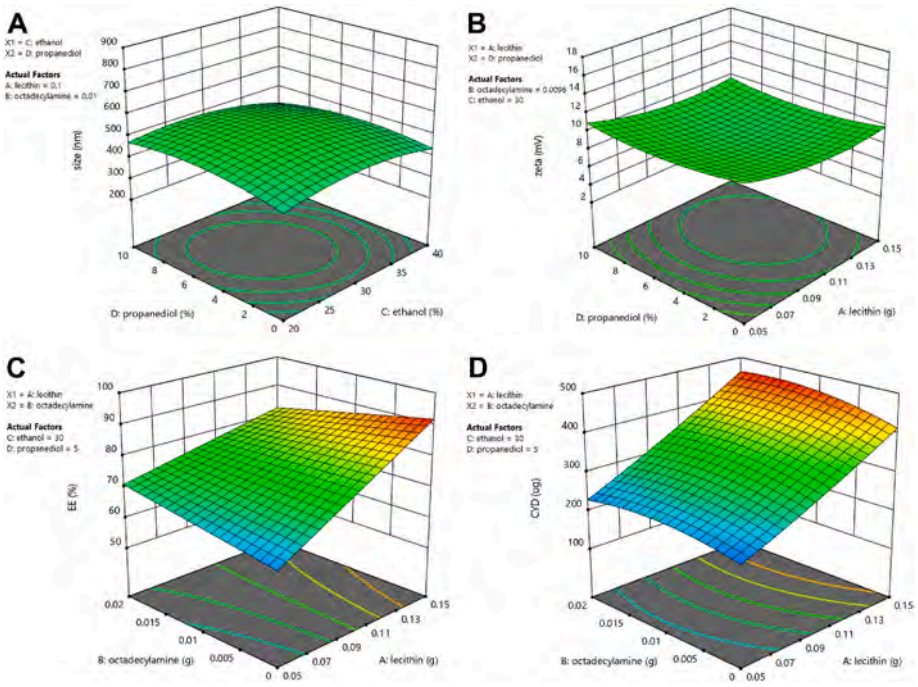

Fig. 1. Three-dimensional response surface plots depicting the effect of the significant variables and interactions between them on the responses of BES (A: particle size; B: zeta potential; C: EE; D: CDR_{24h}).

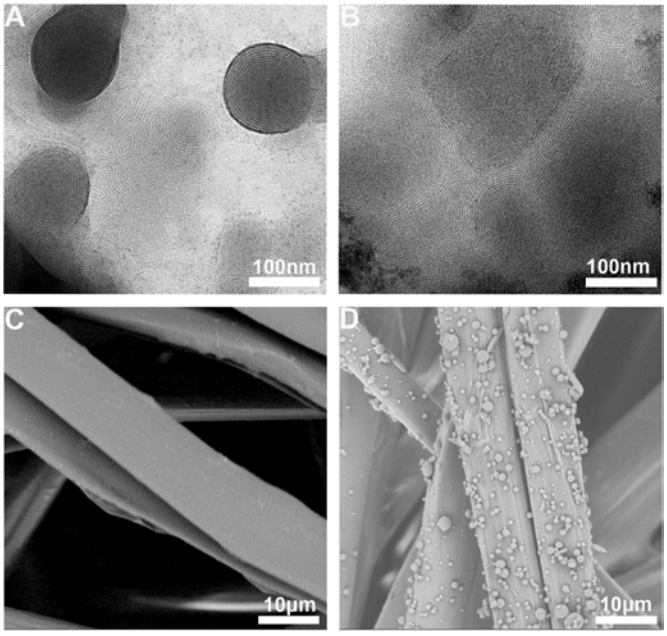

Fig. 2. TEM images of blank BES (A), TEM image of CL@BES (B), SEM image of SFM (C), and SEM image of TDDP (D).

$Y_3 = +77.00 + 10.09A\text{-}0.3329B\text{-}0.3676C\text{-}0.9990D\text{-}4.42AB+0.8075AC+3.08AD\text{-}4.36BC+1.17BD+5.26CD$; $R^2 = 0.8627$

The linear term A (lecithin dosage, $p < 0.001$) and the interaction term CD (the interaction between ethanol and propanediol, $p = 0.0252$) have a significant impact on the encapsulation efficiency. The positive sign of the linear term coefficient A proves the positive influence of the dosage of lecithin on the response value Y_3, and the positive sign of the interaction term coefficient CD proves the positive influence of the interaction between ethanol and propanediol on the response value Y_3. As mentioned above, the main component of lipids in BES is lecithin, and its dosage has a huge impact on the formation of vesicles. The drug used in this study is CL, which is a lipophilic drug. The greater the dosage of phospholipid, the greater the bilayer of phospholipid formed, and the greater the dissolution of lipophilic drugs, which improves the EE of the drug [22]. As a co-solvent, the higher the ethanol content, the more lipophilic drugs are dissolved in the core of the BES. At the same time, the fluidity of the BES membrane increases, and the drug encapsulated in the vesicle is more likely to escape. The higher concentration of ethanol may also dissolve lecithin to destroy the phospholipid bilayer, and the EE may also be reduced [23]. The addition of propanediol at an appropriate concentration reduces the fluidity of the lipid bilayer and can improve the sealing performance of the BES. While too high a concentration of propanediol will increase the particle size of the alcohol and reduce its stability [24].

3.1.4. *Effect of independent variables on cumulative drug release*

The drug release test in vitro was used to observe the release of drug preparations in vivo when simulating a specific medication route. During preliminary experiments, we found that the solubility of CL in PBS was low, resulting in some precipitation, due to that CL is a lipid-soluble small molecule. SDS is an anionic surfactant that is stable in aqueous solution. With the existence of SDS, the solubility of CL in PBS can be improved significantly as previously reported [25], which can avoid the precipitation of CL in the release medium and thus allows for more accurate detection of the amount of CL released. Therefore, we used SDS-PBS as the release medium of CL in this study. The in vitro cumulative drug release of CL@BES in 24 h is between 181.32 ± 38.44–479.17 ± 43.49 μg. The polynomial equation of the model expressed as a coding factor is as follows:

$Y_4 = +345.67 + 106.72A + 14.65B + 1.00C + 2.34D+9.03AB\text{-}0.7905AC\text{-}26.35AD\text{-}15.09BC+9.53BD\text{-}22.91CD+6.78A^2\text{-}21.71B^2+0.4077C^2\text{-}15.85D^2$; $R^2 =$ 0.9584

The linear term A (lecithin dosage, $p < 0.0001$) has a significant effect on the drug release in vitro. The positive sign of the coefficient A of the linear term proves the positive effect of the dosage of lecithin on the response value Y_4. It is reasonable the dosage of lecithin has a significant

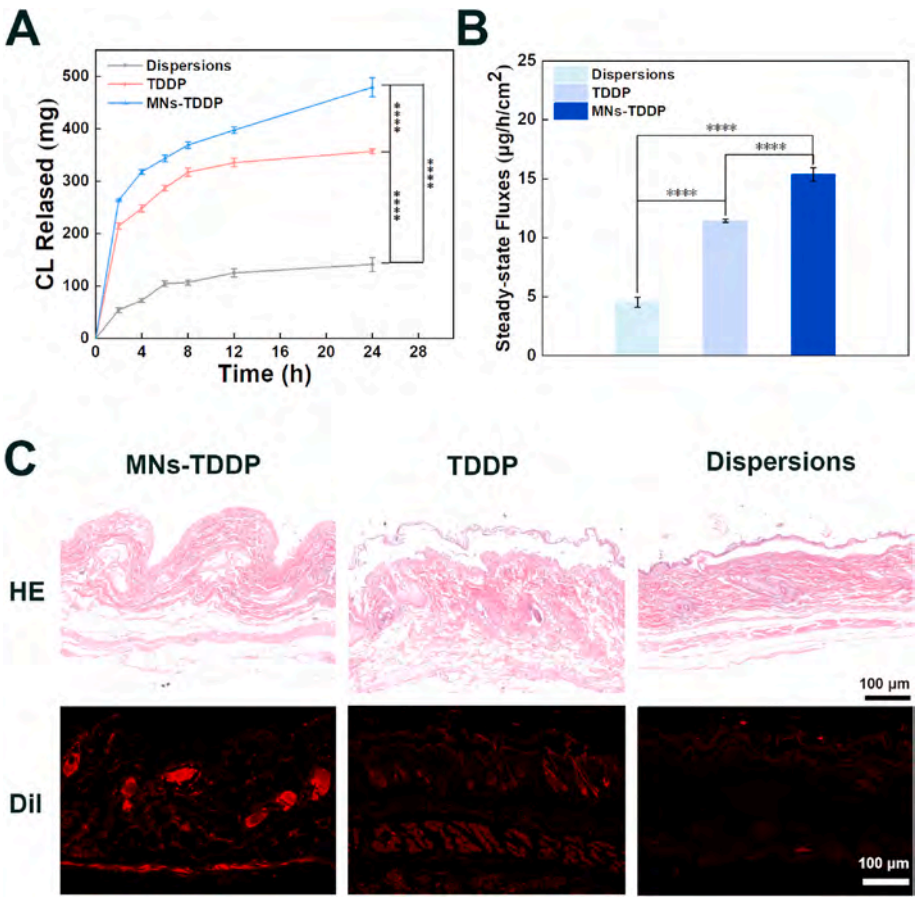

Fig. 3. In vitro transdermal data. A: cumulative drug release curve; B: Steady-state release flux; C: hematoxylin/eosin stainning and fluorescence analysis of the skin sections; Data are expressed as mean ± SD (n ≥ 3), ****$p < 0.0001$.

impact on the loading of the drug, since it has a significant impact on the drug encapsulation rate as mentioned above. The higher the dosage of lecithin, the higher the drug loading and the higher the release of drugs [26]. In addition, the better the sealing of the phospholipid bilayer (affected by ethanol and propanediol) the slower the drug leakage. The presence of ethanol in the BES membrane may lead to the formation of temporary hydrophilic pores on the membrane, resulting drug leakage from the pores, thereby increasing the cumulative drug release [27].

3.1.5. Optimal formula

The above data were processed and optimized using the BBD model of Design Expert 11 (Stat-Ease Inc., USA) to process and optimize the obtained data to obtain the best BES formula. The optimized plan is based on the smallest particle size, the largest zeta potential, the largest EE, and the highest CDR. The optimized formula for BES is as follows: 0.10 g lecithin, 0.01 g octadecylamine, 20% v/v ethanol, 10%v/v propanediol. The corresponding data under the optimized formula are: particle size 506.5 ± 50.85 nm, potential 11.30 ± 1.00 mV, EE 73.50 ± 2.51%, and CDR_{24h} 361.04 ± 38.91 μg. The PDI of the optimized BES is 0.348, within the acceptable range of less than 0.5 [28].

3.2. Characterization of TDDP

The average fiber diameter of SFM is about 10 μm (Fig. 2C). The hydrophilicity of SFM has been significantly increased compared with that of raw cocoon shells ($p < 0.0001$) (Fig. S1). Also, the strain performance of SFM (Fig. S2) is close to 50%, much better than that of the electrospun silk fibroin fibers (less than 7% as reported previously [29]). With better hydrophilic and tensile properties, SFM is a good candidate for the substrate material of transdermal patches. The CL@BES-loaded microspheres have a diameter of about 600 nm and are evenly distributed on the SFM (Fig. 2D). The loading of CL@BES-loaded microspheres in TDDP is also confirmed by the infrared spectra (Fig. S3).

3.3. Skin permeation performance of TDDP

The biggest obstacle to transdermal drug delivery is the dense SC on the skin surface. It is composed of a water-soluble hygroscopic mixture rich in free amino acids, amino acid derivatives and inorganic salts and neatly arranged and dense keratinocytes, which protects the human body from external microorganisms and is the first barrier of human immunity [30]. The SC also prevents most drugs from entering the body through the skin to exert their effects [31]. BES have good transdermal ability and can penetrate the skin more efficiently with the assistance of solid metal MNs which damage the SC and open the skin gap. As shown in Fig. 3A, the transdermal drug release curves have a biphasic release characteristic, that is, the drugs were released rapidly within 2 h, and then entered a slow release phase until 24 h, which may be related to the penetration theorem: concentration difference on both sides of the skin promotes the migration and penetration of drugs from the side with high concentration to the side with low concentration. The greater the concentration difference, the higher the penetration rate. The cumulative transdermal release amounts of free CL, TDDP and MNs-TDDP at 24 h was 141.36 ± 13.11 μg, 357.12 ± 4.60 μg and 479.72 ± 18.30 μg, respectively. The cumulative transdermal release amounts of TDDP was more than 2.5 times that of free CL ($p < 0.0001$), while MNs-TDDP showed an even better performance on transdermal delivery of CL than TDDP did ($p < 0.0001$). The trend of steady-state flux is similar to that of cumulative release (Fig. 3B). These results indicate that the package of BES is great beneficial to CL penetrating through the skin due

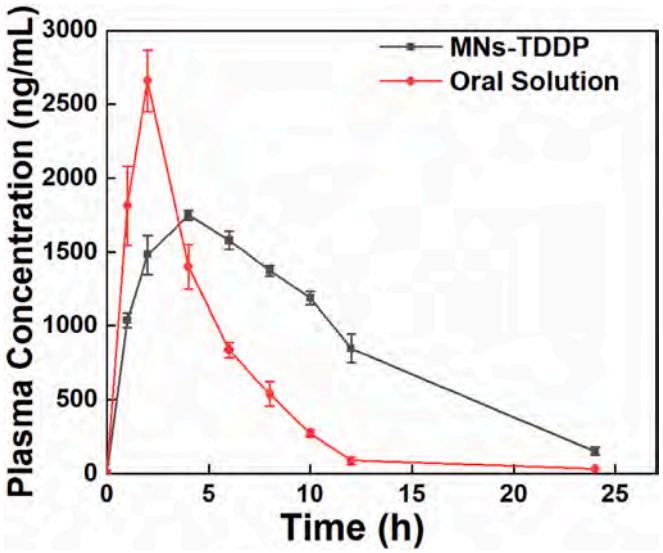

Fig. 4. Profiles of CL levels in plasma with time after oral or TDDP administration.

Table 3
Pharmacokinetics parameters of TDDP and oral administration.

Pharmacokinetics parameter	Oral administration	MNs-TDDP
C_{max} (ng/mL)	2658.63	1749.44
T_{max} (h)	2	4
$T_{1/2}$ (h)	3.63	4.77
k_{el} (h^{-1})	0.190	0.145
$AUC_{(0\text{-}24)}$(ng · min/mL)	12702.53	21895.45
$AUC_{(0\text{-}\infty)}$(ng · min/mL)	12867.05	22950.01

Notes: h = hours; C_{max} = peak plasma concentration; T_{max} = time to reach peak plasma concentration; AUC = area under curve; $T_{1/2}$ = half life; k_{el} = elimination rate constant.

to the joint penetration enhancement effect of ethanol and propanediol [32]. BES enter into the skin by dissolving lipids of SC or pass through gaps smaller than its own size through deformation [33]. DiI-labeled BES was found to enter the skin in large quantities (Fig. 3C). As shown in Fig. 3C, the TDDP-treated skins showed a relatively loose SC compared with the free CL-treated one, which may be related to a dynamic interaction between BES and the SC [34]. Furthermore, MNs-TDDP showed a better transdermal drug delivery effect than TDDP did, which should be mainly due to the following two factors: (1) the conical depression on the skin caused by the MNs which makes BES easier to stay and store in the surface of the skin [35]; (2) the thickness of the local SC treated by the MNs can be reduced, which makes BES easier to pass through, greatly improving their penetration efficiency [36]. As shown in Fig. 3C, the use of MNs did not damage the dermis cells, they only penetrated the part of the epidermis without nerves and blood vessels, and won't cause bleeding, pain and infection [37,38].

3.4. Pharmacodynamic analysis

Fig. 4 shows the fluctuation of CL level in plasma with time after oral or MNs-TDDP administration. The pharmacokinetic parameters of MNs-TDDP and oral administration are shown in Table 3. The CL concentration in plasma reached the maximum at 2 h after oral administration with a C_{max} of 2658.63 ng/ml. While the maximum for MNs-TDDP administration was at 4 h with a C_{max} of 1749.44 ng/ml. The T_{max} value of the MNs-TDDP group was higher than that of the oral group, which should be due to that the barrier function of the skin delayed the penetration of drug and its sustained release from the BES [8]. In contrast, oral administration is equivalent to immediate release of the drug, so the absolute value of the rising and falling slopes in the plasma drug concentration-time curve is very large. Compared with oral administration, transdermal administration effectively prolongs the action time of the drug in vivo [39]. The reason may be that the transdermal administration avoids the first-pass effect of oral administration, and can continuously deliver drugs to the blood circulation. It can be inferred that the duration of the effective blood drug concentration depends on the initial drug loading of the TDDP, that is, if the initial drug loading is increased, the blood drug concentration could remain longer. Our data suggest that transdermal administration can greatly improves

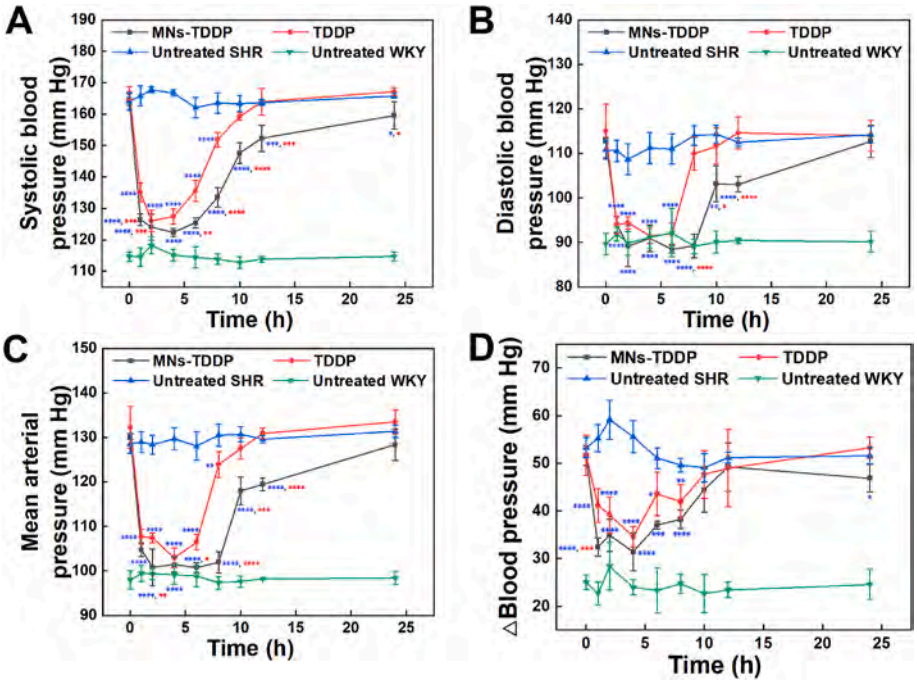

Fig. 5. Changes of SBP (A), DBP (B), MAP (C) and △BP (D) in 24 h after receiving different treatment. SBP: systolic blood pressure; DBP: diastolic blood pressure; MAP: mean arterial pressure; △BP: pulse pressure difference; Data are expressed as mean ± SD (n ≥ 3). *$p < 0.05$, **$p < 0.01$, ***$p < 0.001$ and ****$p < 0.0001$ (blue asterisk refers to comparison with untreated SHR, while red refers to comparison with TDDP). (For interpretation of the references to colour in this figure legend, the reader is referred to the Web version of this article.)

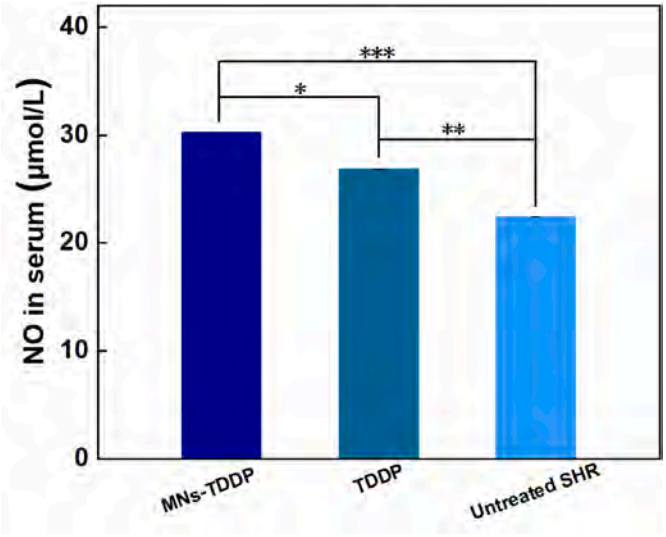

Fig. 6. The concentration of NO in serum after receiving different treatments for 24 h. Data are expressed as mean ± SD (n ≥ 3). *$p < 0.05$, **$p < 0.01$ and ***$p < 0.001$.

the bioavailability of CL, thereby reducing the frequency and dosage of administration, improving patient compliance and reducing costs [40].

3.5. Anti-hypertensive effect of TDDP

SHR is the most studied model animal for cardiovascular diseases related to hypertension [41]. The pathogenesis, complications and hemodynamics of SHR are similar to those of humans, so they are considered to be the animal model closest to human essential hypertension [41]. In this study, SHRs with stable blood pressure were selected for a two-day test to evaluate the antihypertensive effect of TDDP. The untreated SHR and untreated WKY are used as controls. Fig. 5 shows the changes of systolic blood pressure (SBP), diastolic blood pressure (DBP), mean arterial pressure (MAP) and pulse pressure difference (△BP) of the rats from 0 to 24 h. 1–10 h after administration with TDDP, the SBP decreased significantly compared with the untreated SHR control ($p < 0.0001$). Such decline of SBP was greater and lasted much longer in those receiving MNs-TDDP and there are significant differences between MNs-TDDP and TDDP ($p < 0.05$), which may be due to that CL@BES can stay in the skin pores caused by the MNs. In the pores, a number of micro-reservoirs are formed, so that more drugs enter the body and the continuous administration time is also longer [42]. DBP, MAP and △BP among the groups show similar trends as SBP. These results are also consistent with the skin penetration data (Fig. 3). It is worth noting that the curve of DBP is some different from that of SBP, which may be due to that DBP is more sensitive to changes in peripheral vascular resistance than SBP [43–45]. The relatively severe microcirculation disorder in the SHRs may leads to sparse microvessels [46]. The reduction of peripheral vascular resistance after medication is affected by factors such as SHR's microcirculation disorder, which makes the fluctuation of DBP more obvious [47]. Similarly, we speculate that the performance of blood pressure control could be better by increasing the initial drug load of TDDP.

The anti-hypertensive mechanism of CL is related to the concentration of NO in serum [25]. As shown in Fig. 6, MNs-TDDP group had the highest NO level, followed by the TDDP group, and the control had the lowest. Statistical analysis showed that there were significant differences among the three groups although the degree of difference was different. These results have the similar trend with those of blood pressure. The increased NO levels in the two experimental groups confirm the effective delivery of CL via transdermal route, and MNs-TDDP administration has higher transdermal delivery efficiency than TDDP. The performances of anti-hypertensive effect and serum NO is consistent with the data of pharmacokinetic, confirming the significant improvement of the bioavailability of CL via transdermal administration.

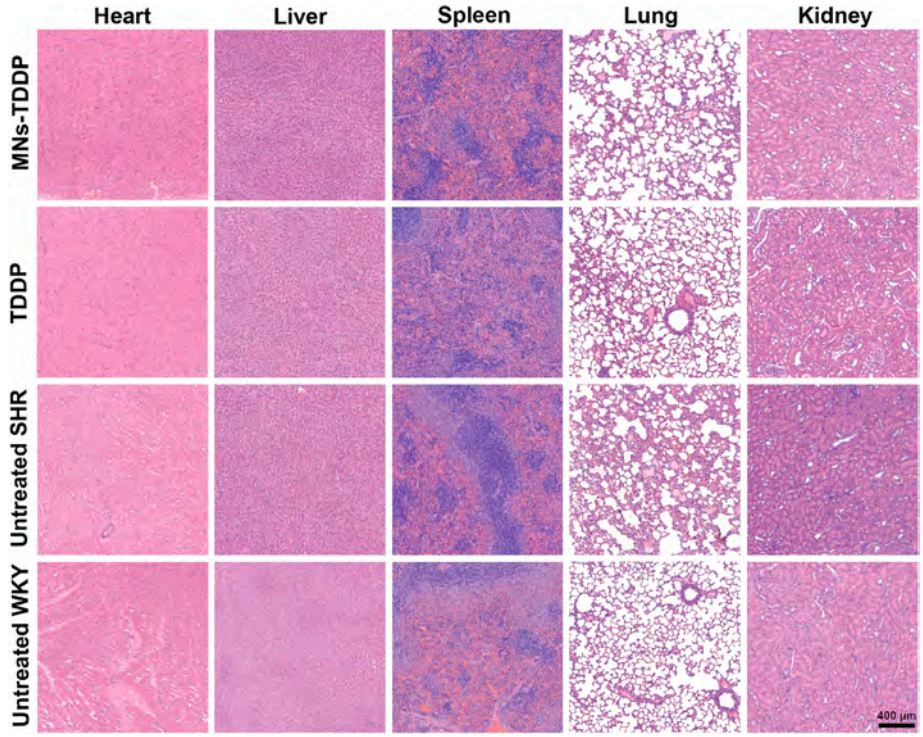

Fig. 7. Micrographs of H&E-stained tissue sections of major organs from the rats after receiving different treatments.

3.6. Histopathological analysis

The biological safety of the TDDP administration was evaluated by hematoxylin/eosin and IF-TUNEL staining assay. As shown in Fig. 7, the main organs (heart, liver, spleen, lung, and kidney) of each group have no obvious local inflammation, and there is no significant difference between experimental groups and control groups. IF-TUNEL data shows that transdermal administration won't cause more apoptosis of major organs compared with controls (Fig. S4). These results indicate that transdermal administration of TDDP has good biological safety, which should be attributed to the good cytocompatibility of ethosomes as previously reported [29,48–50].

4. Conclusion

In this study, the formula of BES was optimized using BBD method. The optimized BES have suitable particle size, positive potential, high encapsulation efficiency and sustained drug release performance. A novel TDDP was obtained by electrospraying the CL@BES-loaded microspheres onto the surface of SFM. TDDP shows a good transdermal performance, and can be further improved significantly with the assistance of MNs. In vivo studies have shown that MNs-TDDP can significantly reduce the fluctuation of plasma CL concentration and increase serum level of NO, thereby lower blood pressure for a longer time, compared with the oral route. These results suggest that the bioavailability of CL can be greatly improved via administration of MNs-TDDP, compared with oral route. Considering its advantages of non-invasiveness, convenience and good biosafety, MNs-TDDP has a good application potential in treating chronic diseases such as hypertension.

CRediT authorship contribution statement

Di Jiang: Conceptualization, Methodology, Investigation, Writing – original draft. **Yuxin Jiang:** Conceptualization, Methodology, Writing-editing. **Kaili Wang:** Methodology, Validation. **Zhe Wang:** Investigation. **Yifei Pei:** Investigation. **Jinglei Wu:** Methodology. **Chuanglong He:** Methodology. **Xiumei Mo:** Conceptualization. **Hongsheng Wang:** Conceptualization, Methodology, Investigation, Writing-editing, Funding acquisition, Supervision.

Declaration of interests

The authors declare that they have no known competing financial interests or personal relationships that could have appeared to influence the work reported in this paper.

Acknowledgements

This research was supported by Science & Technology Commission of Shanghai Municipality (18490740400, 20DZ2254900), the Municipal Public Welfare Research Project (2022AY10001) from Jiaxing, Zhejiang Province and the National Key Research & Development Program of China (2018YFC1706200).

Appendix A. Supplementary data

Supplementary data to this article can be found online at https://doi.org/10.1016/j.jddst.2022.103498.

References

[1] S. Cheng, B. Claggett, A.W. Correia, A.M. Shah, S.D. Solomon, Temporal trends in the population attributable risk for cardiovascular disease the atherosclerosis risk in communities study, Circulation 130 (2014) 820–828.
[2] A. Ahad, M. Aqil, K. Kohli, Y. Sultana, M. Mujeeb, A. Ali, Formulation and optimization of nanotransfersomes using experimental design technique for accentuated transdermal delivery of valsartan, Nanomedicine 8 (2012) 237–249.
[3] C. Panagiotis, Stafylas, A. Pantelis, Sarafidis, Carvedilol in hypertension treatment, Vasc. Health Risk Manag. 4 (2008) 23–30.
[4] T.L. Yue, R.R. Ruffolo, G. Feuerstein, Antioxidant action of carvedilol: a potential role in treatment of heart failure, Heart Fail. Rev. 4 (1999) 39–52.
[5] M. Sharma, R. Sharma, D.K. Jain, A. Saraf, Enhancement of oral bioavailability of poorly water soluble carvedilol by chitosan nanoparticles: optimization and pharmacokinetic study, Int. J. Biol. Macromol. 135 (2019) 246–260.
[6] Y. Tanwar, C. Chauhan, A. Sharma, Development and evaluation of carvedilol transdermal patches, Acta Pharm. 57 (2007) 151–159.
[7] U. Ubaidulla, M.V.S. Reddy, K. Ruckmani, F.J. Ahmad, R.K. Khar, Transdermal therapeutic system of carvedilol: effect of hydrophilic and hydrophobic matrix on in vitro and in vivo characteristics, AAPS PharmSciTech 8 (2007) E13–E20.
[8] H.F. Salem, S.F. El-Menshawe, R.A. Khallaf, Y.K. Rabea, A novel transdermal nanoethosomal gel of lercanidipine HCl for treatment of hypertension: optimization using Box-Benkhen design, in vitro and in vivo characterization, Drug Deliv Transl Res 10 (2020) 227–240.
[9] L.M. Prisant, W.J. Elliott, Drug delivery systems for treatment of systemic hypertension, Clin. Pharmacokinet. 42 (2003) 931–940.
[10] D.-J. Lim, J.B. Vines, H. Park, S.-H. Lee, Microneedles, A versatile strategy for transdermal delivery of biological molecules, Int. J. Biol. Macromol. 110 (2018) 30–38.
[11] J. Yu, Y. Zhang, Y. Ye, R. DiSanto, W. Sun, D. Ranson, F.S. Ligler, J.B. Buse, Z. Gu, Microneedle-array patches loaded with hypoxia-sensitive vesicles provide fast glucose-responsive insulin delivery, Proc. Natl. Acad. Sci. U. S. A. 112 (2015) 8260–8265.
[12] T.M. Tuan-Mahmood, M.T. McCrudden, B.M. Torrisi, E. McAlister, M.J. Garland, T. R. Singh, R.F. Donnelly, Microneedles for intradermal and transdermal drug delivery, Eur. J. Pharmaceut. Sci. 50 (2013) 623–637.
[13] K. Park, Controlled drug delivery systems: past forward and future back, J. Contr. Release 190 (2014) 3–8.
[14] S.H. Abd El-Alim, A.A. Kassem, M. Basha, A. Salama, Comparative study of liposomes, ethosomes and transfersomes as carriers for enhancing the transdermal delivery of diflunisal: in vitro and in vivo evaluation, Int. J. Pharm. 563 (2019) 293–303.
[15] L.N. Shen, Y.T. Zhang, Q. Wang, L. Xu, N.P. Feng, Enhanced in vitro and in vivo skin deposition of apigenin delivered using ethosomes, Int. J. Pharm. 460 (2014) 280–288.
[16] D.M.N. Abouhussein, Enhanced transdermal permeation of BCS class IV aprepitant using binary ethosome: optimization, characterization and ex vivo permeation, J. Drug Deliv. Sci. Technol. 61 (2021), 102185.
[17] G. Nava, E. Piñón, L. Mendoza, N. Mendoza, D. Quintanar, A. Ganem, Formulation and in vitro, ex vivo and in vivo evaluation of elastic liposomes for transdermal delivery of ketorolac tromethamine, Pharmaceutics 3 (2011) 954–970.
[18] F. Torrades, S. Saiz, J. García-Hortal, Using central composite experimental design to optimize the degradation of black liquor by Fenton reagent, Desalination 268 (2011) 97–102.
[19] Y. Yan, H. Zhang, J. Sun, P. Wang, K. Dong, Y. Dong, J. Xing, Enhanced transdermal delivery of sinomenine hydrochloride by ethosomes for anti-inflammatory treatment, J. Drug Deliv. Sci. Technol. 36 (2016) 201–207.
[20] C. Pinilla, P.M. Reque, A. Brandelli, Effect of oleic acid, cholesterol, and octadecylamine on membrane stability of freeze-dried liposomes encapsulating natural antimicrobials, Food Bioprocess Technol. 13 (2020) 599–610.
[21] X. Luo, M. Liu, L. Hu, Q. Qiu, X. Liu, L. Cong, L. Mei, L. Yang, T. Zhang, S. Zhou, Targeted delivery of pixantrone to neutrophils by poly(sialic acid)-p-octadecylamine conjugate modified liposomes with improved antitumor activity, Int. J. Pharm. 547 (2018) 315.
[22] L. Tunyaluk, B. Prapaporn, K. Pasarat, A. Thanaporn, Ethosomes of phenylethyl resorcinol as vesicular delivery system for skin lightning applications, BioMed Res. Int. 2017 (2017), 8310979.
[23] K. Pathak, A. Varma, N. Akhtar, Ethosomes as vesicles for effective transdermal delivery: from bench to clinical implementation, Curr. Clin. Pharmacol. 11 (2016) 168–190.
[24] A. Gupta, S. Singh, N.G. Kotla, T. Webster, Formulation and evaluation of a topical niosomal gel containing a combination of benzoyl peroxide and tretinoin for antiacne activity, Int. J. Nanomed. 10 (2015) 171–182.
[25] N.M. Sallam, R.A.B. Sanad, M.M. Ahmed, E.L.S. Khafagy, M. Ghorab, S. Gad, Impact of the mucoadhesive lyophilized wafer loaded with novel carvedilol nano-spanlastics on biochemical markers in the heart of spontaneously hypertensive rat models, Drug Deliv. Transl. Res. 11 (2021) 1009–1036.
[26] Goindi, Kumar Shishu, Kaur Gautam, Amanpreet, Novel flexible vesicles based topical formulation of levocetirizine: in vivo evaluation using oxazolone-induced atopic dermatitis in murine model, J. Liposome Res. 24 (2014) 249–257.
[27] S. Ahmed, M.A. Kassem, S. Sayed, Bilosomes as promising nanovesicular carriers for improved transdermal delivery: construction, in vitro optimization, ex vivo permeation and in vivo evaluation, Int. J. Nanomed. 15 (2020) 9783–9798.
[28] P. Mura, M. Bragagni, N. Mennini, M. Cirri, F. Maestrelli, Development of liposomal and microemulsion formulations for transdermal delivery of clonazepam: effect of randomly methylated β-cyclodextrin, Int. J. Pharm. 475 (2014) 306–314.
[29] X. Song, H. Hong, G.E. Fawal, J. Wu, D. Jiang, K. Wang, Y. Jiang, C. He, X. Mo, H. Wang, Transcutaneous tumor vaccination combined with aPD-1 treatment produces a synergistic antitumor effect, Acta Biomater. 140 (2022) 247–260.
[30] K. Ita, Transdermal Iontophoretic Drug Deliv.: Adv. Chall. 24 (2016) 386–391.
[31] A. Azeem, N. Jain, Z. Iqbal, F.J. Ahmad, M. Aqil, S. Talegaonkar, Feasibility of proniosomes-based transdermal delivery of frusemide: formulation optimization

and pharmacotechnical evaluation, Pharmaceut. Dev. Technol. 13 (2008) 155–163.
[32] S.N. Park, H.J. Lee, H.S. Kim, M.A. Park, H.A. Gu, Enhanced transdermal deposition and characterization of quercetin-loaded ethosomes, Kor. J. Chem. Eng. 30 (2012) 688–692.
[33] Yang Hengjia, Wu Xuanjin, Zhou Zhongzheng, Chen Xiguang, Kong Ming, Enhanced transdermal lymphatic delivery of doxorubicin via hyaluronic acid based transfersomes/microneedle complex for tumor metastasis therapy, Int. J. Biol. Macromol. 125 (2018) 9–16.
[34] J.P. Zhang, Y.H. Wei, Y. Zhou, Y.Q. Li, X.A. Wu, Ethosomes, binary ethosomes and transfersomes of terbinafine hydrochloride: a comparative study, Arch Pharm. Res. (Seoul) 35 (2012) 109–117.
[35] A. Ahad, A.A. Al-Saleh, A.M. Al-Mohizea, F.I. Al-Jenoobi, M. Raish, A.E.B. Yassin, M.A. Alam, Pharmacodynamic study of eprosartan mesylate-loaded transfersomes Carbopol((R)) gel under Dermaroller((R)) on rats with methyl prednisolone acetate-induced hypertension, Biomed. Pharmacother. 89 (2017) 177–184.
[36] Y.C. Kim, J.H. Park, M.R. Prausnitz, Microneedles for drug and vaccine delivery, Adv. Drug Deliv. Rev. 64 (2012) 1547–1568.
[37] M.R. Zare, M. Khorram, S. Barzegar, B. Sarkari, Q. Asgari, S. Ahadian, K. Zomorodian, Dissolvable carboxymethyl cellulose/polyvinylpyrrolidone microneedle arrays for transdermal delivery of Amphotericin B to treat cutaneous leishmaniasis, Int. J. Biol. Macromol. 182 (2021) 1310–1321.
[38] N. Dabholkar, S. Gorantla, T. Waghule, V.K. Rapalli, A. Kothuru, S. Goel, G. Singhvi, Biodegradable microneedles fabricated with carbohydrates and proteins: revolutionary approach for transdermal drug delivery, Int. J. Biol. Macromol. 170 (2021) 602–621.
[39] H. Yang, X. Wu, Z. Zhou, X. Chen, M. Kong, Enhanced transdermal lymphatic delivery of doxorubicin via hyaluronic acid based transfersomes/microneedle complex for tumor metastasis therapy, Int. J. Biol. Macromol. 125 (2019) 9–16.
[40] J.P. Appleton, K. Krishnan, P.M. Bath, Transdermal delivery of glyceryl trinitrate: clinical applications in acute stroke, Expet Opin. Drug Deliv. 17 (2020) 297–303.
[41] Y. Li, F. Liu, C. Su, B. Yu, D. Liu, H.J. Chen, D.A. Lin, C. Yang, L. Zhou, Q. Wu, W. Xia, X. Xie, J. Tao, Biodegradable therapeutic microneedle patch for rapid antihypertensive treatment, ACS Appl. Mater. Interfaces 11 (2019) 30575–30584.
[42] F.J. Verbaan, S.M. Bal, D.J. van den Berg, J.A. Dijksman, M. van Hecke, H. Verpoorten, A. van den Berg, R. Luttge, J.A. Bouwstra, Improved piercing of microneedle arrays in dermatomed human skin by an impact insertion method, J. Contr. Release 128 (2008) 80–88.
[43] J.L.M.L.L.M.L. le Noble, G.J. Tangelder, D.W. Slaaf, H.V. Essen, R.S. Reneman, H. Struyker-Boudier, A functional morphometric study of the cremaster muscle microcirculation in young spontaneously hypertensive rats, J. Hypertens. 8 (1990) 741.
[44] H.S. Boudier, N.J. Le, M.W. Messing, M.S. Huijberts, N.F. Le, E.H. Van, The microcirculation and hypertension, Hypertension Suppl. 10 (1992) 147–156.
[45] G.L. Baumbach, D.D. Heistad, Remodeling of cerebral arterioles in chronic hypertension, Hypertension 13 (1989) 968.
[46] B.I. Levy, G. Ambrosio, A.R. Pries, H. Struijker-Boudier, Microcirculation in hypertension: a new target for treatment? Circulation 104 (2001) 735–740.
[47] S.E. Brett, J.M. Ritter, P.J. Chowienczyk, Diastolic blood pressure changes during exercise positively correlate with serum cholesterol and insulin resistance, Circulation 101 (2000) 611–615.
[48] X. Yang, X. Wang, H. Hong, G. Elfawal, S. Lin, J. Wu, Y. Jiang, C. He, X. Mo, G. Kai, H. Wang, Galactosylated chitosan-modified ethosomes combined with silk fibroin nanofibers is useful in transcutaneous immunization, J. Contr. Release 327 (2020) 88–99.
[49] L. Ma, X. Wang, J. Wu, D. Zhang, L. Zhang, X. Song, H. Wang, Polyethylenimine and sodium cholate-modified ethosomes complex as multidrug carriers for thetreatment of melanoma through transdermal delivery, Nanomedicine 14 (2019) 2395–2408.
[50] H. Hong, X. Wang, X. Song, G.E. Fawal, K. Wang, D. Jiang, Y. Pei, Z. Wang, H. Wang, Transdermal delivery of interleukin-12 gene targeting dendritic cells enhances the anti-tumour effect of programmed cell death protein 1 monoclonal antibody, Biomater. Transl. 2 (2021) 151–164.